

Hierarchical Phase Space Structure of Dark Matter Haloes: Tidal debris, Caustics, and Dark Matter annihilation

Niayesh Afshordi,^{1,*} Roya Mohayaee,^{2,†} and Edmund Bertschinger^{3,‡}

¹*Perimeter Institute for Theoretical Physics, 31 Caroline St. N., Waterloo, ON, N2L 2Y5, Canada*

²*Institut d'Astrophysique de Paris, CNRS, UPMC, 98 bis boulevard Arago, France*

³*Department of Physics and Kavli Institute for Astrophysics and Space Research, MIT
Room 37-602A, 77 Massachusetts Ave., Cambridge, MA 02139, USA*

(Dated: August 9, 2021)

Most of the mass content of dark matter haloes is expected to be in the form of *tidal debris*. The density of debris is not constant, but rather can grow due to formation of *caustics* at the apocenters and pericenters of the orbit, or decay as a result of phase mixing. In the phase space, the debris assemble in a hierarchy which is truncated by the primordial temperature of dark matter. Understanding this phase structure can be of significant importance for the interpretation of many astrophysical observations and in particular dark matter detection experiments. With this purpose in mind, we develop a general theoretical framework to describe the hierarchical structure of the phase space of cold dark matter haloes. We do not make any assumption of spherical symmetry and/or smooth and continuous accretion. Instead, working with correlation functions in the action-angle space, we can fully account for the hierarchical structure (predicting a two-point correlation function $\propto \Delta J^{-1.6}$ in the action space), as well as the primordial discreteness of the phase space. As an application, we estimate the boost to the dark matter annihilation signal due to the structure of the phase space within virial radius: the boost due to the hierarchical tidal debris is of order unity, whereas the primordial discreteness of the phase structure can boost the total annihilation signal by up to an order of magnitude. The latter is dominated by the regions beyond 20% of the virial radius, and is largest for the recently formed haloes with the least degree of phase mixing.

I. INTRODUCTION

Cosmological N-body simulations show that dark matter (DM) haloes which form in a Λ CDM Universe contain a large number of subhaloes of all sizes and masses. What remains outside the subhaloes are ungrouped individual particles whose masses set the resolution limit of the simulation. If the simulations were to have enough resolution to resolve every single subhalo then it is expected that the smallest subhaloes would be the microhaloes of about $10^{-6} M_{\odot}$ [1, 2, 3]. Does all the mass of a given halo reside inside the gravitationally bound subhaloes? As a subhalo falls through the gravitational field of its host halo, it becomes tidally disrupted. A tidal stream extends along the orbit of the subhalo and can contain a large fraction of the satellite mass. Therefore, a significant fraction of a DM halo is expected to be in the form of *streams* and *caustics*. Depending on their length, the density of the streams can vary and is relatively not very large. However, as a stream folds back on itself, zones of higher density, *i.e.* caustics, form (see *e.g.* [4, 5, 6, 7, 8]). In principle, these are not true caustics but only smeared-out caustics due to finite DM velocity dispersion, however, it is convenient to refer to them simply as DM caustics. Hereafter we shall refer to unbound streams and caustics jointly as *tidal debris*.

Dark matter tidal debris, so far mostly unresolved in cosmological N-body simulations, are expected to populate our own halo. Many stellar counterparts to such debris have been detected so far (*e.g.* [9, 10]) and many more are expected to be detected with future missions like GAIA. The hierarchical growth of the host halo from the disruption of satellite haloes reflects in a hierarchical structure of the phase space. The true lowest cutoff to this hierarchy is not set by the microhaloes but by primordial dark matter velocity dispersion. The hierarchical phase structure indicates that after removing all bound subhaloes from a given DM halo, its phase space remains still unsmooth due to debris from disrupted subhaloes. The tidal debris are never smeared out because of conservation of phase space density and volume, although they become less dense as they wrap around the halo. It is this phase structure which we study here.

Secondary infall or self-similar accretion model provides a solid theoretical base for the study of halo formation, and models the phase structure of DM haloes [11, 12]. However, since this model assumes continuous accretion, it cannot capture the hierarchical nature of halo formation. On the other hand, numerical simulations still lack enough resolution to resolve the hierarchical phase structure, although progress is being made in this direction [8, 13, 14].

Here, we aim at capturing the hierarchical phase structure of dark matter haloes and its intrinsically discrete nature, without resorting to any assumption of spherical symmetry or smooth and self-similar accretion. We divide the structure of a dark matter halo into three categories: (1) the primordial and intrinsically discrete phase

*Electronic address: nafshordi@perimeterinstitute.ca

†Electronic address: roya@iap.fr

‡Electronic address: edbert@mit.edu

structure, formed prior to any merger or accretion and entirely due to the coldness of the initial condition; (2) the hierarchical phase structure of tidal debris from disrupted satellites, and (3) the hierarchical phase structure of undisrupted subhaloes. We leave the study of the undisrupted substructures to a companion paper [15] and in this work we only study cases (1) and (2).

To study phase structure induced by debris from disrupted satellites, we assume that at a given level in the hierarchy, all structures added earlier and which lie at smaller scales are smooth. This sets the lowest level of the hierarchy at the scale determined by the velocity dispersion of earliest dark matter haloes. However, this is not entirely correct since the earliest dark matter haloes themselves are not smooth and have a structure which is due to the coldness of the initial condition. Thus, there is a fundamental discreteness scale which is determined by primordial dark matter velocity dispersion (see Fig. 1).

This complicated process is studied here through correlation functions in the action-angle space where Hamiltonian is only a function of the adiabatic invariants, *i.e.* the action variables. Their conjugate variables, *the angle variables* increase linearly in time. The action-angle variables are extremely useful for studying tidal streams [16, 17, 18, 19, 20]. However, working with the action-angle variables, we are restricted to regions within the virial radius (with a quasi-static potential), and hence the phase structures that might arise outside the virial radius (*e.g.* between the virial and the turnaround radii) cannot be studied in the present framework. For direct DM detection and cosmic-ray signal of DM annihilation, only the nearby phase structure plays a rôle and our method is valid (see *e.g.* [21]). However, for lensing experiments and γ -ray emission from DM annihilations, for example from other galaxies, the structures outside the virial radius can be rather important (see *e.g.* [22]).

We assume that the satellite orbits are integrable in the host DM potential (although, in V we remark on chaos and non-integrable systems). Therefore, the phase space distribution can be described in terms of the action-angle variables, $\{J_i, \theta_i\}$, so that:

$$\dot{\theta}_i = \frac{\partial \mathcal{H}}{\partial J_i} = \Omega_i, \quad (1)$$

$$\dot{J}_i = -\frac{\partial \mathcal{H}}{\partial \theta_i} = 0, \quad (2)$$

where the Hamiltonian, $\mathcal{H} = \mathcal{H}[J]$, is only a function of action variables, \mathbf{J}_i and Ω_i s are the angular frequencies. Fig. (2) shows a cartoon picture of phase mixing in the action-angle space, and its correspondence to the real space.

The hierarchical phase structure and its *fundamental* discreteness set by primordial DM velocity dispersion are captured by the correlation function of the phase density. Since, after a long time, the distribution in the angle space is uniform, the phase density is only a function of the action variables. This can be easily seen by writing

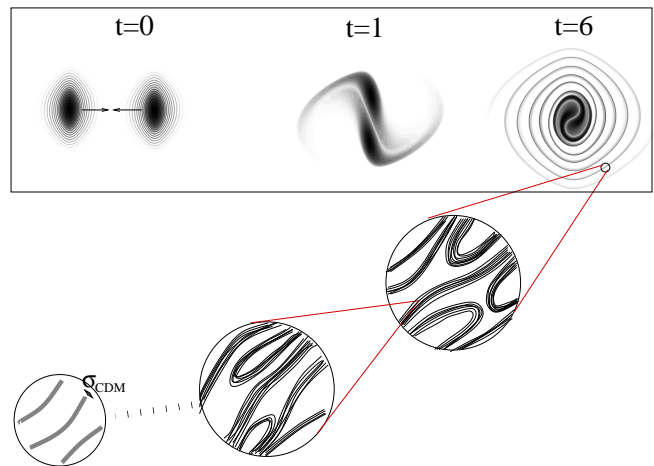


FIG. 1: The top horizontal panel shows the phase space of the merger of two dark matter haloes, each of which has its own hierarchy of phase structure. The times on the top panel refer to the crossing times. The zooming shows that each hierarchy contains a lower level and so on. The hierarchy is cut at the scale of the smallest dark matter halo that has been accreted to the final halo. However, the phase space is not smooth below this scale. Indeed, the phase space is intrinsically discrete due to the coldness of dark matter shown by the last zooming on the left. (Top panel: courtesy of Vlasov-Poisson simulation [23].)

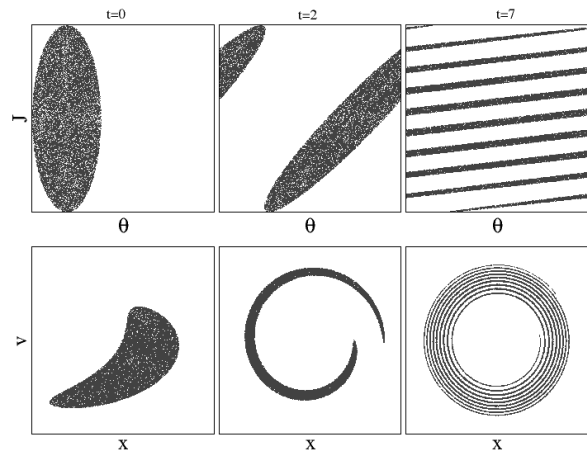


FIG. 2: A one dimensional cartoon of the evolution of tidal streams in both phase and action-angle spaces. As structure wraps around the phase space, more streams cross the same angle coordinate, which leads to a discrete lattice-like structure in the action space.

the collisionless Boltzmann equation for the equilibrium distribution in the action-angle space:

$$\frac{\partial f}{\partial t} + \dot{\theta}_i \frac{\partial f}{\partial \theta_i} + \dot{J}_i \frac{\partial f}{\partial J_i} = 0, \quad (3)$$

which, combining with Eq. (2), implies that the equilibrium phase space density can only be a function of action

variables (and is known as the *strong Jeans theorem* [24]).

This enables us to evaluate the density-density correlation function. Our results are only valid statistically for typical haloes and thus may not agree with results obtained for individual haloes in the simulations.

The nature of DM remains a mystery. Supersymmetry and extra-dimensional extensions of the standard electroweak model provide a natural candidate in the form of a weakly interacting and massive particle (hereafter WIMP). These species should fill up the galactic halo. If DM consists of WIMP's, they are expected to strongly annihilate in the dense regions of our halo and generate in particular gamma-rays and charged cosmic rays. Hence, hierarchical structure of phase space can lead to the enhancement of DM annihilation signal [25]. We also evaluate the boost to the annihilation signal due to tidal debris and discreteness of the phase structure. We show that the boost due to tidal debris is of order one, whereas the boost from the discrete phase structure can be up to one order of magnitude higher.

In Section II we review a few basic relations for action-angle variables. In Section III A and III B, we describe the correlation functions that would account for the phase structure due to tidal debris and their discreteness. In Section IV A, we evaluate the boost on the annihilation signal due to tidal debris. In Section IV B, we evaluate the boost of the annihilation signal from intrinsic discreteness of the phase structure, and finally Section V concludes the paper.

II. STREAMS AND COHERENCE VOLUME OF THE PHASE SPACE

We use the definition of action-angle variables (2) and assume that the frequencies are not degenerate, *i.e.* the Hessian matrix

$$\mathcal{H}_{ij} \equiv \frac{\partial^2 \mathcal{H}}{\partial J_i \partial J_j} = \frac{\partial \Omega_i}{\partial J_j}, \quad (4)$$

has non-zero eigenvalues, or equivalently, a non-vanishing determinant:

$$|\mathcal{H}_{ij}| \neq 0, \quad (5)$$

with the possible exception of a zero measure region of the phase space. Note that, this implies that the halo potential cannot be assumed to be exactly spherically symmetric, as two of the frequencies would be equal.

If a satellite galaxy has originally a small spread in the action variables, ΔJ_i , its spread in the angle variables increases as:

$$\Delta \theta_i = (\mathcal{H}_{ij} \Delta J_j) t_{acc,p} + \Delta \theta_0, \quad (6)$$

where $t_{acc,p}$ is the time since accretion of the progenitor of the debris into the halo. The last term, the initial extent of the debris, is subdominant at large times. We set this term to zero for now, but at the end of Section

IV B, we discuss when it can become important and how it could affect our results. Therefore, the total volume swept in the angle space grows as

$$\Delta^3 \theta = (|\mathcal{H}_{ij}| \Delta^3 J) t_{acc,p}^3 = (\Delta^3 \Omega) t_{acc,p}^3 \quad (7)$$

where we used the definition of \mathcal{H}_{ij} in equation (4), and $\Delta^3 \Omega$ is the volume occupied by the debris of satellite particles in the frequency space.

As the total volume of the angle space is $(2\pi)^3$, the number of streams passing through each angular coordinate is

$$N_{\text{stream}} = (\Delta^3 \Omega) \left(\frac{t_{acc,p}}{2\pi} \right)^3. \quad (8)$$

Thus, the total mass of each stream, m_{stream} , is the mass of the debris, m , divided by N_{stream}

$$m_{\text{stream}} = \frac{m}{N_{\text{stream}}} = \left(\frac{m}{\Delta^3 \Omega} \right) \left(\frac{t_{acc,p}}{2\pi} \right)^{-3}. \quad (9)$$

Put another way, the action space is divided into cells of volume:

$$\Delta^3 J_{\text{stream}} = \left(\frac{2\pi}{t_{acc,p}} \right)^3 |\mathcal{H}_{ij}|^{-1}, \quad (10)$$

as a result of phase space mixing (*e.g.* [19]).

With this picture in mind, we can write the distribution in the action space as the sum of the contributions from individual progenitors:

$$f(\mathbf{J}, \theta) = \sum_p f_p(\mathbf{J}, \theta; t_{acc,p}), \quad (11)$$

where each f_p has a cellular structure characterized by Eq. (10), as shown in Fig. (3), which gets finer and finer with time. Eq. (11) is the phase space analog of the widely used *halo model* in cosmology [26, 27], where the density is assumed to be the sum of contributions from individual haloes with given profiles. Correspondingly, f_p characterizes the profile of individual progenitors in our picture.

We can now write the real space density as:

$$\begin{aligned} \rho(\mathbf{x}, t) &= \sum_p \int d^3 J d^3 \theta f_p(\mathbf{J}, \theta; t_{acc,p}) \delta_D^3[\mathbf{x} - \tilde{\mathbf{x}}(\mathbf{J}, \theta)] \\ &= \sum_p \int d^3 J \tilde{f}_p(\mathbf{J}, \mathbf{x}, t_{acc,p}) \tilde{\rho}(\mathbf{x}; \mathbf{J}), \end{aligned} \quad (12)$$

where $\tilde{\rho}(\mathbf{x}; \mathbf{J})$ is the density of a distribution of unit mass, with a fixed action variable \mathbf{J} , and uniform angle distribution:

$$\tilde{\rho}(\mathbf{x}; \mathbf{J}) \equiv \int \frac{d^3 \theta}{(2\pi)^3} \delta_D^3[\mathbf{x} - \tilde{\mathbf{x}}(\theta, \mathbf{J})], \quad (13)$$

while

$$\tilde{f}_p(\mathbf{J}, \mathbf{x}, t_{acc,p}) \equiv \tilde{\rho}(\mathbf{x}; \mathbf{J})^{-1} \int \frac{d^3 \theta}{(2\pi)^3} f_p(\mathbf{J}, \theta, t_{acc,p}) \delta_D^3[\mathbf{x} - \tilde{\mathbf{x}}(\theta, \mathbf{J})]. \quad (14)$$

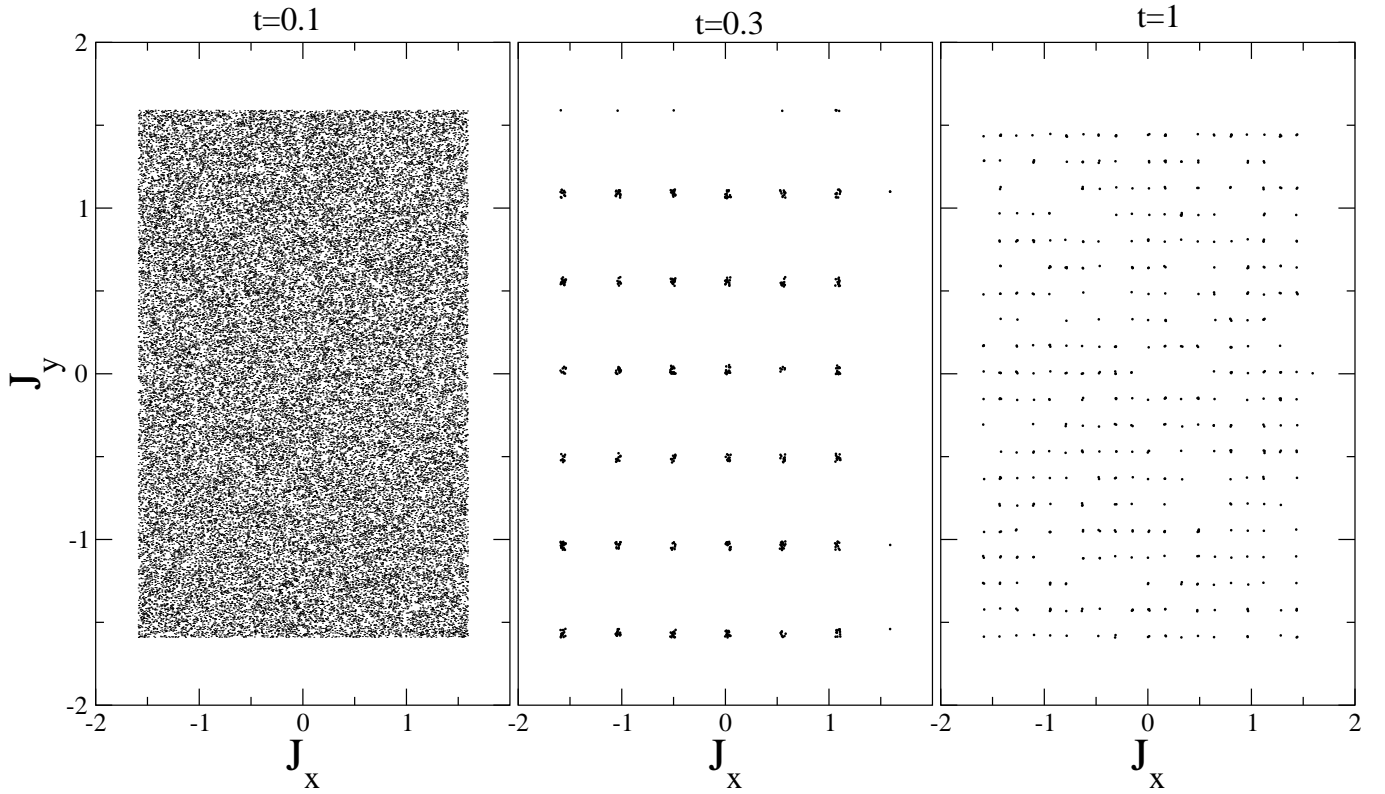


FIG. 3: The action-space distribution of debris in a unit 2d torus with unit particle mass and no potential. The debris is originally within $0 < x, y < 0.1$, and $-10 < v_x, v_y < 10$. The figures show a cut through the action space with $0.09 < x, y < 0.1$, which is characterized by $\tilde{f}_p(\mathbf{J}, \mathbf{x}, t_{acc,p})$ (Eq. 14) in our formalism.

An example of \tilde{f}_p is shown in Fig. (3) for debris in a toy model of a unit torus. As we will explicitly show in IV A, projecting this discrete structure in the action space of the debris into the real space leads to discrete, (nearly) singular, caustics that are only smoothed by the original velocity dispersion of the progenitor.

III. CLUSTERING IN THE PHASE SPACE

Averaging over different possible realizations of the debris within a halo, the mean phase space density can be written as an integral:

$$\langle \sum_p \tilde{f}_p(\mathbf{J}, \mathbf{x}, t_{acc,p}) \rangle = \int dN_p g^{(1)}(\mathbf{J} - \mathbf{J}_p, \mathbf{x}, t_{acc,p}), \quad (15)$$

where $g^{(1)}$ and \mathbf{J}_p are the profile and mean action of individual progenitors, while

$$dN_p \equiv dm_p d^3 J_p dt_{acc,p} \frac{dn}{dm_p d^3 J_p dt_{acc,p}} \quad (16)$$

is the differential progenitor number density per units of progenitor mass, m_p , its action space volume $d^3 J_p$, and its accretion time $t_{acc,p}$. We now follow an analogy with the cosmological halo model[26, 27] to write the clustering

in the action space as a superposition of one and two-progenitor terms:

$$\begin{aligned} & \left\langle \sum_{p_1, p_2} \tilde{f}_{p_1}(\mathbf{J}_1, \mathbf{x}, t_{acc,p_1}) \tilde{f}_{p_2}(\mathbf{J}_2, \mathbf{x}, t_{acc,p_2}) \right\rangle \\ &= \int dN_p (1 - \text{prog.}) + \int dN_{p_1} \int dN_{p_2} (2 - \text{prog.}). \quad (17) \end{aligned}$$

The one-progenitor term characterizes the self-clustering of individual progenitor action-space profiles.

$$(1 - \text{prog.}) = g^{(1)}(\mathbf{J}_1 - \mathbf{J}_p, \mathbf{x}, t_{acc,p}) g^{(1)}(\mathbf{J}_2 - \mathbf{J}_p, \mathbf{x}, t_{acc,p}), \quad (18)$$

while the two-progenitor terms characterize the correlation between phase space density at different action variables, within different progenitors:

$$\begin{aligned} (2 - \text{prog.}) &= g^{(2)}(\mathbf{J}_1 - \mathbf{J}_{p_1}, \mathbf{J}_2 - \mathbf{J}_{p_2}, \mathbf{x}, t_{acc,p_1}, t_{acc,p_2}) \\ &= g_{\text{con.}}^{(2)}(\mathbf{J}_1 - \mathbf{J}_{p_1}, \mathbf{J}_2 - \mathbf{J}_{p_2}, \mathbf{x}, t_{acc,p_1}, t_{acc,p_2}) \\ &+ g^{(1)}(\mathbf{J}_1 - \mathbf{J}_{p_1}, \mathbf{x}, t_{acc,p_1}) g^{(1)}(\mathbf{J}_2 - \mathbf{J}_{p_2}, \mathbf{x}, t_{acc,p_2}). \quad (19) \end{aligned}$$

In the limit that the mean actions of different progenitors are not correlated, the connected part of the (2-prog.) term goes to zero: $g_{\text{con.}}^{(2)} \rightarrow 0$, and thus the two-progenitor term reduces to the correlation within the smooth halo.

Note that this limit cannot be strictly realized, as due to phase space conservation, phase streams tend to avoid each other, leading to $g^{(2)} < 0$ at small separations $\mathbf{J}_{p_1} - \mathbf{J}_{p_2}$. However, Liouville's theorem is not valid for coarse-grained phase space density, and thus coarse-grained progenitors can overlap in the action space.

The connected part of the two-progenitor term originates from the clustering of the initial conditions of the progenitors of the host halo, which is generally expected from the clustering of cosmological haloes. However, the structure of the one-progenitor term is more subtle: In addition to the cellular structure described in the previous section (Fig. 3), the internal structure of each progenitor prior to its accretion onto the host halo would introduce a hierarchy within each cell. In fact, in a hierarchical picture of structure formation, one expects the sub-cellular structure of the one-progenitor term to be inherited from the two-progenitor terms within progenitors prior to their accretion onto the main halo (see Fig. 1). The key difference between the two hierarchies, however, is that phase mixing only continues in the action space of the main halo, and (following the tidal disruption) has stopped in the action spaces of the progenitors.

For statistically self-similar initial conditions, we expect the sub-cellular and two-progenitor terms to blend into one roughly self-similar structure in the action space, although individual realizations have periodic structures with the characteristic volume given in Eq. (10). We provide a scaling ansatz for this structure in III A. However, the self-similarity is cut-off by the free streaming of dark matter particles on small separations, due to their finite intrinsic velocity dispersion. This is responsible for the fundamental discreteness of the phase space distribution (see Fig. 1), which we model in III B.

A. hierarchical phase structure from tidal debris

We first consider the phase structures due to tidal debris. Once again, we emphasize that these are the tidal streams that have fallen into the gravitational field of the host halo and are no longer bound to the original satellite.

The first level of approximation that we will use to study phase space clustering of cold dark matter (CDM) is to assume a (statistically) hierarchical formation history, where any trace of the cold initial conditions has been wiped out through phase mixing. Furthermore, we ignore the possibility of gravitationally bound structures in this paper (see the companion paper [15] on this subject). The impact of cold initial conditions will be addressed in subsequent sections.

Assuming *uniform distribution in angles* (or complete phase mixing), the density at each point in the halo is given by:

$$\rho(\mathbf{x}) = (2\pi)^3 \int d^3J f(\mathbf{J}) \tilde{\rho}(\mathbf{x}; \mathbf{J}), \quad (20)$$

where $f(\mathbf{J})$ is the phase space density, while $\tilde{\rho}(\mathbf{x}; \mathbf{J})$ was defined in Eq. (13). Note that in (20), the function $\tilde{\rho}$ has the dimension of inverse volume, $1/V(\mathbf{J})$.

We shall assume adiabatic invariance; the action remains constant as new structures are added on larger scales. Hence, the distribution function in the action space, $f(\mathbf{J})$, does not change with time, except when new structures are added due to satellites that are newly accreted inside the virial radius.

The assumption of uniformity in the angle space allows us to separate the effect of phase mixing from that of hierarchical structure formation. While the former is the cause of original caustic formation, too much phase mixing (within a fixed potential) will eventually smooth out the real space density distribution. The assumption of a smooth $f(\mathbf{J})$ distribution, implies that phase mixing is complete.

On the other hand, the effect of hierarchical structure formation is captured in $f(\mathbf{J})$, through the fact that structure in $f(\mathbf{J})$ is added on different scales, at different times in the history of the halo. A statistical measure of this history is the two point correlation function of the action space density. We thus hypothesize that the correlation function:

$$\xi_f(\mathbf{J}_1, \mathbf{J}_2) \equiv \langle f(\mathbf{J}_1) f(\mathbf{J}_2) \rangle \quad (21)$$

should be a power law for statistically self-similar initial conditions:

$$\langle f(\mathbf{J}_1) f(\mathbf{J}_2) \rangle_{\text{debris}} \simeq A |\bar{\mathbf{J}}|^{-\alpha} |\mathbf{J}_1 - \mathbf{J}_2|^{-\alpha}, \quad (22)$$

as long as $|\mathbf{J}_1 - \mathbf{J}_2| \ll |\bar{\mathbf{J}}|$ with $\bar{\mathbf{J}} = (\mathbf{J}_1 + \mathbf{J}_2)/2$. The form of the correlation function uses the symmetry between \mathbf{J}_1 and \mathbf{J}_2 . It also guarantees that small scale structures are captured, as structures are added on different scales at different times (see Figs. 1 for demonstration). Moreover, since actions remain constant in the adiabatic invariance approximation $dA/dt \simeq 0$ on small scales. In other words, the correlation function $\xi_f(\mathbf{J}_1, \mathbf{J}_2)$ grows inside-out in the $\mathbf{J}_1, \mathbf{J}_2$ space.

The mean phase space density of a virialized halo, assuming a virial overdensity of ~ 200 , is given by:

$$(2\pi)^3 \Delta^3 J \sim r_{\text{vir}}^3 \sigma_{\text{vir}}^3 \sim \frac{(GM)^2}{10H} \quad (23)$$

$$\Rightarrow \langle f(\mathbf{J}) \rangle \sim \frac{10H}{G^2 M}, \quad (24)$$

where M is the halo virial mass. The virial action variable is also roughly:

$$J_{\text{vir}} \sim r \sigma_{\text{vir}} \sim \frac{(GM)^{2/3}}{(10H)^{1/3}}. \quad (25)$$

Given that $M \propto a^{6/(n_{\text{eff}}+3)}$ and $H \propto a^{-3/2}$ when perturbations grow during the matter-dominated era, with a being the cosmological scale factor, and n_{eff} the slope of the linear power spectrum, we conclude:

$$\langle f(\mathbf{J}) \rangle \propto J^{-\frac{3(n_{\text{eff}}+7)}{n_{\text{eff}}+11}} \Rightarrow \alpha = \frac{3(n_{\text{eff}}+7)}{n_{\text{eff}}+11} \simeq 1.6 \pm 0.1, \quad (26)$$

where we have assumed $n_{\text{eff}} \simeq -2.5 \pm 0.5$ for cosmological haloes.

An alternative way to derive (26) is to consider the self-similar collapse models of Fillmore & Goldreich [11], where they calculate the actions and use adiabatic invariance to find the outcome of spherical cold secondary infall in an Einstein-de Sitter universe. For the spherical self-similar linear initial condition of

$$\frac{\delta M}{M} \Big|_{\text{init.}} \propto M^{-\varepsilon}, \quad (27)$$

they find the action at the turn-around radius scales as

$$J_{ta} \propto M_{ta}^{\varepsilon+1/3} t_{ta}^{\frac{2}{3\varepsilon}-\frac{1}{3}}, M_{ta} \propto t_{ta}^{\frac{2}{3\varepsilon}} \quad (28)$$

for $\varepsilon < 2/3$, where M_{ta} is the mass within the turn-around radius. Although (28) is only for the radial action, and the two other action variables vanish due to spherical symmetry, one may imagine that for triaxial CDM haloes, the three actions would become comparable: $J_\phi \sim J_\theta \sim \varepsilon J_r \sim \varepsilon J_{ta}$, where ε characterizes the triaxiality of the halo (not to be confused with the self-similar profile index ε in (27)). Therefore, eliminating time from the two equations in (28), the phase space density, $f(\mathbf{J})$ scales as:

$$f(\mathbf{J}) \sim \frac{M_{ta}}{J_{ta}^3} \sim J_{ta}^{\frac{6}{3\varepsilon+4}}. \quad (29)$$

Assuming that the self-similar linear density profile has the same radial/mass scaling as the variance of the cosmological density fluctuations, $\sigma(M) \propto M^{-(n_{\text{eff}}+3)/6}$ yields $\varepsilon \simeq (n_{\text{eff}} + 3)/6$ ($< 2/3$ for CDM Harrison-Zel'dovich primordial power spectrum), which, plugging into (29), reproduces (26).

B. fundamental discreteness of the phase space structure

In the previous section, we considered the hierarchical addition of tidal debris to a DM halo. However, the hierarchy has a lower cut-off set by the velocity dispersion of the smallest accreted satellite. Micro haloes of $\sim 10^{-6}$ solar mass could indeed determine such a cut-off [1, 2, 3]. However, this cutoff is far above the primordial velocity dispersion of DM itself. Therefore, the primordial velocity dispersion introduces a *fundamental* discreteness in the phase structure. In other words, the smooth phase space distribution of the last section ignores the discrete nature of multiple streams in the phase space due to the presence of a cut-off in the CDM hierarchy. This discreteness shows up as a cellular or lattice structure in the action space, with a characteristic cell volume given in (10) (see Figs. 2 and 3 for 1d and 2d cartoons; More realistic simulated examples are discussed in [19]). After averaging over different spacings, expected for different accretion times of different debris, the discreteness would

only show up as the zero-lag of the action space correlation function:

$$\langle f(\mathbf{J}_1)f(\mathbf{J}_2) \rangle_{\text{dis}} \simeq \frac{m_{\text{stream}}^2}{\Delta^3 J_{\text{stream}}} \delta_D^3(\mathbf{J}_1 - \mathbf{J}_2) \quad (30)$$

where m_{stream} and $\Delta^3 J_{\text{stream}}$ were defined in equations (9-10), and here we have assumed a zero initial temperature for CDM particles. A finite CDM temperature will smoothen the delta function, as the phase space density cannot exceed its primordial value (see Fig. 1 for a cartoon).

IV. EXAMPLE: DARK MATTER ANNIHILATION MEASURE

A. DM annihilation in tidal debris

In this subsection, we consider the enhancement in the expectation value of the annihilation measure due to hierarchical structures built in the phase space from tidal debris.

For a uniform distribution in the angle space, the expectation value of the annihilation measure is given by:

$$\begin{aligned} \Phi &= \int d^3x \langle \rho(\mathbf{x})^2 \rangle \\ &= (2\pi)^6 \int d^3J_1 d^3J_2 \xi_f(\mathbf{J}_1, \mathbf{J}_2) \int d^3x \tilde{\rho}(\mathbf{x}; \mathbf{J}_1) \tilde{\rho}(\mathbf{x}; \mathbf{J}_2). \end{aligned} \quad (31)$$

We remark that the above integral can also be relevant for the direct detection of DM, as it quantifies the variance of the density field.

In order to investigate the impact of caustics, near the apocenters and pericenters of the orbits, we make a simple analogy with a one-dimensional harmonic oscillator:

$$H = \frac{1}{2}(p_x^2 + p_y^2 + p_z^2) + \frac{1}{2}\omega^2 x^2, \quad (32)$$

For concreteness, we also assume the other two dimensions are compact with the length L_y and L_z , although the Hamiltonian has no explicit dependence on y and z coordinates. As the evolution in the three spatial directions decouple, we can simply read off three action variables from the areas of phase diagrams for each direction:

$$J_x = \frac{p_x^2}{2\omega} + \frac{1}{2}\omega x^2, \quad (33)$$

$$J_y = \frac{L_y p_y}{2\pi}, J_z = \frac{L_z p_z}{2\pi}. \quad (34)$$

From these relations, we can find $\tilde{\rho}(\mathbf{x}; \mathbf{J})$ using its definition in Eq. (13):

$$\tilde{\rho}(\mathbf{x}; \mathbf{J}) = \frac{(x_{\text{max}} - x_{\text{min}})}{\pi V \sqrt{(x - x_{\text{min}})(x_{\text{max}} - x)}}, \quad (35)$$

where

$$x_{\max} = -x_{\min} = \sqrt{2J_x/\omega}, \quad (36)$$

$$V = L_y L_z (x_{\max} - x_{\min}). \quad (37)$$

Notice that the square root singularity in the projection kernel $\tilde{\rho}(\mathbf{x}; \mathbf{J})$ is very similar to the singularity expected near CDM caustics. However, for a smooth distribution in the action-space $f(\mathbf{J})$, the real space density $\rho(\mathbf{x})$ is an integral over the kernel (Eq. 20), which would lead to a smooth $\rho(\mathbf{x})$. Therefore, a discrete distribution in the action space is necessary to produce caustic singularities in the real space (otherwise known as fold catastrophes or Zel'dovich pancakes).

We then notice that the toy model of Eq. (32) is similar to the motion in a nearly spherical potential, in the sense that the motion in one direction (x or radial) is limited by requiring constant action variables, while the two other directions (y and z, or angular directions) are compact. Based on this analogy, we will use:

$$\tilde{\rho}(\mathbf{x}; \mathbf{J}) \sim \frac{[r_{\max}(\mathbf{J}) - r_{\min}(\mathbf{J})]}{V(\mathbf{J})\sqrt{[r - r_{\min}(\mathbf{J})][r_{\max}(\mathbf{J}) - r]}}, \quad (38)$$

where we have assumed an integrable nearly-spherical potential, with small angular momentum (and third integral), while $V(\mathbf{J})$ is the spatial volume occupied by the stream of action \mathbf{J} . The radii, r_{\min} and r_{\max} are the minimum and maximum radii of all orbits with the same action variable. However, the general structure of the singularity close to boundaries does not change in other geometries.

Using Eq. (38), we can evaluate the x integral in the emission measure (31). For $\mathbf{J}_1 \simeq \mathbf{J}_2$, the integral is logarithmically divergent around $r \simeq r_{\max}(\mathbf{J}_1) \simeq r_{\max}(\mathbf{J}_2)$ as well as $r \simeq r_{\min}(\mathbf{J}_1) \simeq r_{\min}(\mathbf{J}_2)$. Focussing on the outer caustic r_{\max} we find:

$$\int d^3x \tilde{\rho}(\mathbf{x}; \mathbf{J}_1) \tilde{\rho}(\mathbf{x}; \mathbf{J}_2) \simeq \frac{4\pi r_{\max}^2 (r_{\max} - r_{\min})}{V^2(\mathbf{J}_1)} \times \cosh^{-1} \left| \frac{r_{\max}(\mathbf{J}_1) + r_{\max}(\mathbf{J}_2)}{r_{\max}(\mathbf{J}_1) - r_{\max}(\mathbf{J}_2)} \right| \quad (39)$$

This yields:

$$\int d^3x \tilde{\rho}(\mathbf{x}; \mathbf{J}_1) \tilde{\rho}(\mathbf{x}; \mathbf{J}_2) \sim V(\mathbf{J})^{-1} \left| \ln \left(\frac{F^i \Delta J_i}{|\bar{\mathbf{J}}|} \right) \right|, \quad (40)$$

where $F^i \sim \frac{1}{4} |\bar{\mathbf{J}}| \partial \ln r_{\max} / \partial J_i$ and can be calculated, given the gravitational potential of the host halo. Therefore, the annihilation measure takes the form:

$$\Phi \sim A \int d^3 \bar{\mathbf{J}} |\bar{\mathbf{J}}|^{-\alpha} \int d^3 \Delta \mathbf{J} |\Delta \mathbf{J}|^{-\alpha} \left| \ln \left(\frac{F |\Delta \mathbf{J}|}{|\bar{\mathbf{J}}|} \right) \right|. \quad (41)$$

We see that since $3 - \alpha > 0$, the integral is finite and dominated by large ΔJ 's. The boost to the annihilation signal, which is introduced by small scale clustering in

the action space (*i.e.* that $\alpha > 0$) is thus given by:

$$1 + B_{\text{debris}} \equiv \frac{\Phi}{\Phi_{\text{smooth}}} \simeq \frac{\int d^3 \bar{\mathbf{J}} V(\bar{\mathbf{J}})^{-1} \bar{\mathbf{J}}^{-\alpha} \int d^3 \Delta \mathbf{J} |\Delta \mathbf{J}|^{-\alpha} \left| \ln \left(\frac{F |\Delta \mathbf{J}|}{|\bar{\mathbf{J}}|} \right) \right|}{\int d^3 \bar{\mathbf{J}} V(\bar{\mathbf{J}})^{-1} \bar{\mathbf{J}}^{-2\alpha} \int d^3 \Delta \mathbf{J} \left| \ln \left(\frac{F |\Delta \mathbf{J}|}{|\bar{\mathbf{J}}|} \right) \right|} \simeq \frac{9}{(\alpha - 3)^2} F^\alpha = \mathcal{O}(1), \quad (42)$$

given that $F \sim \partial \ln r_{\max} / \partial \ln J$ is a dimensionless number of order unity.

Therefore, we see that the boost factor obtained here for the tidal debris is dominated by larger separations, as seen from expression (42) whereas our approximation (38) is valid for small separations. To emphasize, (38) is valid in the vicinity of caustics whereas the integral (42) demonstrates that most contributions come from large separations in the action space.

To summarize, while we predict an $\mathcal{O}(1)$ boost in annihilation signal due to (finite separation) clustering in action space, the main effect comes from large structures (and not caustics) which are not accurately captured in our framework. In the next section, we will address the impact of the discreteness of the phase space of CDM haloes.

B. DM annihilation boost due to discreteness of phase structures and catastrophes

The primordial velocity dispersion of DM induces a fundamental discreteness in the hierarchical phase structure and can enhance the annihilation signal. The emission measure due to this discreteness is calculated by inserting (30) in expression (31). Summing over all streams and subtracting the smooth part which is obtained by smoothing over the fundamental streams, we obtain

$$\delta \Phi_{\text{dis}} = \sum_{\text{stream}} m_{\text{stream}}^2 \times \int d^3x [\tilde{\rho}(\mathbf{x}; \mathbf{J}_{\text{stream}})^2 - \tilde{\rho}(\mathbf{x}; \mathbf{J}_{\text{stream}})_{\text{smooth}}^2] \simeq K^2 \left(\frac{t}{2\pi} \right)^{-3} \int d^3\Omega \left(\frac{dM_{\text{halo}}}{d^3\Omega} \right)^2 \times \int d^3x [\tilde{\rho}(\mathbf{x}; \mathbf{J})^2 - \tilde{\rho}(\mathbf{x}; \mathbf{J})_{\text{smooth}}^2], \quad (43)$$

for the enhancement of the emission measure due to discreteness of the phase structure, where $\tilde{\rho}(\mathbf{x}; \mathbf{J})_{\text{smooth}}$ is the stream density, smoothed to the level that different streams overlap, and for the stream mass we assume:

$$m_{\text{stream}} \sim K \frac{dM_{\text{halo}}}{d^3\Omega} \left(\frac{t}{2\pi} \right)^{-3}, \quad (44)$$

where $d^3\Omega$ is the volume element in the frequency space and factor K is the ratio of the density of debris to that of the host halo: $\rho_{\text{debris}} = m/v \sim K \rho_{\text{halo}}$.

The above expression is to be compared to the annihilation measure for the smooth halo:

$$\begin{aligned} \Phi_{\text{smooth}} &= \int d^3\Omega \left(\frac{dM_{\text{halo}}}{d^3\Omega} \right) \\ &\times \int d^3\Omega' \left(\frac{dM_{\text{halo}}}{d^3\Omega'} \right) \int d^3x \tilde{\rho}(\mathbf{x}; \mathbf{J}) \tilde{\rho}(\mathbf{x}; \mathbf{J}'), \end{aligned} \quad (45)$$

where Ω and Ω' are functions of \mathbf{J} and \mathbf{J}' respectively. Therefore, the boost associated with a given point in the action space is given by:

$$\begin{aligned} B_{\text{dis}}[\mathbf{J}] &\equiv \frac{\delta\Phi_{\text{dis}}}{\Phi_{\text{smooth}}} = \\ K^2 \left(\frac{t}{2\pi} \right)^{-3} &\frac{\left(\frac{dM_{\text{halo}}}{d^3\Omega} \right) \int d^3x [\tilde{\rho}(\mathbf{x}; \mathbf{J})^2 - \tilde{\rho}(\mathbf{x}; \mathbf{J})_{\text{smooth}}^2]}{\int d^3\Omega' \left(\frac{dM_{\text{halo}}}{d^3\Omega'} \right) \int d^3x \tilde{\rho}(\mathbf{x}; \mathbf{J}) \tilde{\rho}(\mathbf{x}; \mathbf{J}')} \end{aligned} \quad (46)$$

In order to estimate the boost factor, we should first approximate the density integral $\int d^3x \tilde{\rho}(\mathbf{x}; \mathbf{J}) \tilde{\rho}(\mathbf{x}; \mathbf{J}')$. As we discussed in the previous section for $|\mathbf{J} - \mathbf{J}'| \ll |\mathbf{J}|$ the integral is dominated by the regions around the turn-around radii (or caustics) and thus grows as

$$\int d^3x \tilde{\rho}(\mathbf{x}; \mathbf{J}) \tilde{\rho}(\mathbf{x}; \mathbf{J}') \sim \frac{|\ln(|\mathbf{J} - \mathbf{J}'|/|\mathbf{J}|)|}{V(\mathbf{J})}, \quad (47)$$

as seen in Eq. (40). In the opposite limit, $|\mathbf{J} - \mathbf{J}'| \sim |\mathbf{J}|$, assuming that the two density kernels overlap, $\tilde{\rho}(\mathbf{x}; \mathbf{J})$ can be approximated as roughly constant, which yields:

$$\int d^3x \tilde{\rho}(\mathbf{x}; \mathbf{J}) \tilde{\rho}(\mathbf{x}; \mathbf{J}') \sim V^{-1}(\mathbf{J}). \quad (48)$$

Now we note that in (46), the integral over Ω' (or equivalently J') in the denominator is dominated by the large values of $|\mathbf{J} - \mathbf{J}'|$, while the numerator is in the small $|\mathbf{J} - \mathbf{J}'|$ regime. Therefore, substituting from (47-48), we find:

$$\begin{aligned} B_{\text{dis}}[\mathbf{J}] &\simeq K^2 \left(\frac{t}{2\pi} \right)^{-3} \left| \frac{d \ln M_{\text{halo}}}{d^3\Omega} \right| \left| \ln \left(\frac{|\Delta\mathbf{J}_{\text{CDM}}|}{|\Delta\mathbf{J}_{\text{int-stream}}|} \right) \right| \\ &= K^2 \frac{1}{3} \left(\frac{t}{2\pi} \right)^{-3} \left| \frac{d \ln M_{\text{halo}}}{d^3\Omega} \right| \ln \left(\frac{f_{\text{CDM}}}{\langle f_{\text{halo}} \rangle} \right), \end{aligned} \quad (49)$$

where $|\Delta\mathbf{J}_{\text{CDM}}|$ and $|\Delta\mathbf{J}_{\text{int-stream}}|$ characterise the fundamental CDM stream width and the inter-stream spacing, respectively. The stream thickness and spacing in real space have been calculated within the framework of selfsimilar model [28]. However to obtain the ratio we use a far simpler approximation. To get the last line of expression (49), we have used the fact that the volume in phase space occupied by the fundamental streams is

$(2\pi)^3 \Delta^3 \mathbf{J}_{\text{CDM}} = M_{\text{halo}}/f_{\text{CDM}}$, while the total volume in phase space of the entire halo is: $(2\pi)^3 \Delta^3 \mathbf{J}_{\text{int-stream}} = M_{\text{halo}}/\langle f_{\text{halo}} \rangle$.

The logarithmic enhancement factor is roughly:

$$\frac{1}{3} \ln \left(\frac{f_{\text{CDM}}}{\langle f_{\text{halo}} \rangle} \right) \simeq 20 + \ln \left(\frac{m_\chi}{100 \text{ GeV}} \right), \quad (50)$$

for CDM particles of mass m_χ . In arriving at (50) we have used that $f_{\text{CDM}} \sim \Omega_m \rho_{\text{crit}} (T_\chi/T_{\text{CMB}})^3 / \sigma_{\text{CDM}}^3$ and $\langle f_{\text{halo}} \rangle \sim 10^3 \Omega_m \rho_{\text{crit}} / \sigma_{\text{vir}}^3$, with $T_{\text{CMB}} \sim 10^{-4} \text{ eV}$, $T_\chi = \frac{1}{3} m_\chi \sigma_{\text{CDM}}^2 \sim m_\chi / 40$ is the CDM kinetic decoupling temperature.

In order to estimate the boost factor in (49), we also need to find the volume element occupied in the frequency space, $d^3\Omega$, by a given mass element. First we should notice that for a Keplerian potential $\varphi(r) \propto -r^{-1}$, this volume element vanishes as three frequencies are equal, *i.e.* $\Omega_r = \Omega_\phi = \Omega_3$, where Ω_3 is the frequency for the third integral.

For a general potential, $\varphi(r)$, we have

$$\frac{\Omega_r}{\Omega_\phi} - 1 = \sqrt{3 + \frac{d \ln \varphi'}{d \ln r}} - 1, \quad (51)$$

for a nearly circular orbit and where $'$ indicates first derivative w.r.t. r , *i.e.* $\varphi' = d\varphi/dr$. Moreover, the extent in Ω_3 depends on the triaxiality of the halo:

$$d\Omega_3 \sim \epsilon \Omega_\phi, \quad (52)$$

where $\epsilon \sim 10\%$ characterizes the typical triaxiality of CDM haloes. Therefore, we will approximate the volume element as

$$d^3\Omega \sim 4\pi \epsilon \Omega_\phi^2 \left(\sqrt{3 + \frac{d \ln \varphi'}{d \ln r}} - 1 \right) d\Omega_\phi, \quad (53)$$

where

$$\Omega_\phi^2 \sim \frac{GM_{\text{halo}}}{r^3} = \frac{\varphi'}{r}. \quad (54)$$

Hence, for a general potential we obtain

$$\begin{aligned} \frac{d \ln M_{\text{halo}}}{d^3\Omega} &= \frac{1}{2\pi\epsilon} (2 + d \ln \varphi' / d \ln r) (\varphi' / r)^{-1/2} \\ &\times \left[\left(\sqrt{3 + d \ln \varphi' / d \ln r} - 1 \right) (\varphi' / r - \varphi'') \right]^{-1}, \end{aligned} \quad (55)$$

To evaluate (49) we also need to know the multiplication factor K , which is the ratio of the density of disrupted satellite to that of the host halo. This factor can be evaluated for a general spherical potential, assuming that the debris start with the maximum density that allows them to be tidally unbound:

$$K \simeq 3 (\varphi' - r\varphi'') (2\varphi' + r\varphi'')^{-1} \quad (56)$$

Putting (55) and (56) in (49) we obtain

$$B_{\text{dis}} = 36\pi^2(\varphi' - r\varphi'')(2\varphi' + r\varphi'')^{-1} \left(\sqrt{3 + \tilde{\varphi}} - 1 \right)^{-1} \\ \times (\varphi'/r)^{-3/2} \left(\frac{3}{8\pi G\rho_{\text{crit}}} \right)^{-3/2} \frac{1}{3\epsilon} \ln \left(\frac{f_{\text{CDM}}}{\langle f_{\text{halo}} \rangle} \right) \quad (57)$$

where $\tilde{\varphi} = d(\ln \varphi')/d(\ln r)$ and $\rho_{\text{crit}} = \frac{3H_0^2}{8\pi G}$ is the critical density of the Universe. Moreover, we have used the fact that the product of the present-day Hubble constant and the age of the Universe is unity ($H_0 t = 1.03 \pm 0.04$), for the current concordance cosmology.

For a power-law potential:

$$\varphi(r) = -\varphi_0 r^{-\beta} \quad \beta \neq 1, \quad (58)$$

one can see that (57) yields

$$B_{\text{dis}} = \frac{72\pi^2}{3\epsilon} \frac{(\beta + 2)\sqrt{2(1 - \beta)}}{(\sqrt{2 - \beta} - 1)} \ln \left(\frac{f_{\text{CDM}}}{\langle f_{\text{halo}} \rangle} \right) \left(\frac{3\rho_{\text{halo}}}{\rho_{\text{crit}}} \right)^{-3/2}, \quad (59)$$

where ρ_{halo} , the local halo density for a general potential is

$$\rho(r) = \frac{1}{4\pi G} (\varphi'' + 2\varphi'/r), \quad (60)$$

from Poisson equation.

For the power-law potential (58), we can find the local density in terms of the critical density and the radius and consequently obtain the boost factor (57) as a function of r/r_{vir} where r_{vir} is the virial radius of the halo, defined as the radius within which the mean density is $200\rho_{\text{crit}}$. The local boost factor for a power-law potential, and our nominal values of ϵ and $f_{\text{CDM}}/\langle f_{\text{halo}} \rangle$, is

$$B_{\text{dis}} = \frac{36}{5}\pi^2 \frac{\beta + 2}{(1 - \beta)\sqrt{2 - \beta} - 1} \left(\frac{r}{r_{\text{vir}}} \right)^{3(\beta+2)/2}. \quad (61)$$

The above expression shows that the boost is most significant in the outskirts of the halo, and for large values of β . Indeed, the local boost diverges as $\beta \rightarrow 1$. We note that, in the context of an NFW potential[29]:

$$\varphi_{\text{NFW}} = -\varphi_0 \frac{\ln(1 + x)}{x}, \quad (62)$$

i.e. $\beta \sim 1$ corresponds to the outskirts of the halo and $\beta \sim -1$ to the central part.

Similarly to the power-law potential, we can obtain the local boost factor (57) for an NFW potential (62). The boost is shown in Fig. 4 as a function of r/r_s and for different values of the concentration parameter $c \equiv r_{\text{vir}}/r_s$. The boost increases as we go towards the outskirts of the halo as the number of streams decreases, hence increasing the density of individual caustics. As we increase the concentration, the central density of the halo becomes large, which in turn decreases the local boost factor.

Having evaluated the local boost, we can evaluate the total boost from the halo which we defined as

$$B_{\text{total}} \equiv \frac{\Phi_{\text{total}}}{\Phi_{\text{smooth}}} - 1, \quad (63)$$

where

$$\Phi_{\text{smooth}} = r_s^3 \rho_s^2 \int_0^c 4\pi x^2 \rho(x)^2 dx, \quad (64)$$

and

$$\Phi_{\text{total}} = r_s^3 \rho_s^2 \int_0^c [1 + B_{\text{dis}}(x)] \rho(x)^2 4\pi x^2 dx, \quad (65)$$

where B_{dis} is given by (57) and the density profile of the smooth halo is given by $\rho(x)$. For NFW density profile $\rho = \rho_s/[x(1+x)^2]$ where ρ_s is the scale density, we have plotted the variation of the total boost with the concentration parameter, c , in Fig. (5). Again, the boost decreases as we increase the concentration, since the flux becomes dominated by the central part of the halo.

We saw that the boost is mostly in the outskirts of the haloes, namely beyond the 20% of the virial radius. However, one has to be cautious, since in the outskirts of the halo the gravitational field of the halo approaches a Keplerian potential, causing the frequencies to become degenerate and the term $\Delta\theta_0$ in (6), which we have so far ignored, can become important. Thus, we need to study the importance of this term for our analysis and the boost. Expression (6) now becomes

$$\Delta\theta = t \Delta\Omega \left(1 + \frac{1}{t} \frac{\Delta\theta_0}{\Delta\Omega} \right). \quad (66)$$

Hence the volume element in the angle space (7) should be replaced by

$$\Delta^3\theta = (\Delta^3\Omega) t^3 \det \left(\delta_{ij} + \frac{1}{t} \frac{\partial\theta_{0i}}{\partial\Omega_j} \right). \quad (67)$$

where \det stands for the determinant. For circular orbit approximation we have $\Omega_\phi = \sqrt{\varphi'/r}$ and we use expressions (51) and (52) for volume element in the frequency space. We thus find that the boost (57) has to be multiplied by the inverse of the following determinant:

$$\det \left(\delta_{ij} + \frac{1}{t} \frac{\partial\theta_{0i}}{\partial\Omega_j} \right) \simeq \left(1 + \frac{1}{t\sqrt{\varphi'/r}} \right) \left(1 + \frac{1}{ct\sqrt{\varphi'/r}} \right) \\ \times \left(1 + \frac{1}{t\sqrt{\varphi'/r}(\sqrt{3+\tilde{\varphi}}-1)} \right) \quad (68)$$

if the frequencies were to become near degenerate. In obtaining (68) we have used $\Delta\theta_0/\Delta\Omega \sim 1/\Omega$. The effect of this factor in reducing the boost is shown for an NFW potential (62) by the dashed lines in Figs. 4 and 5. The local boost is reduced slightly in the outskirts as expected and the total boost is reduced by a factor of about 2.

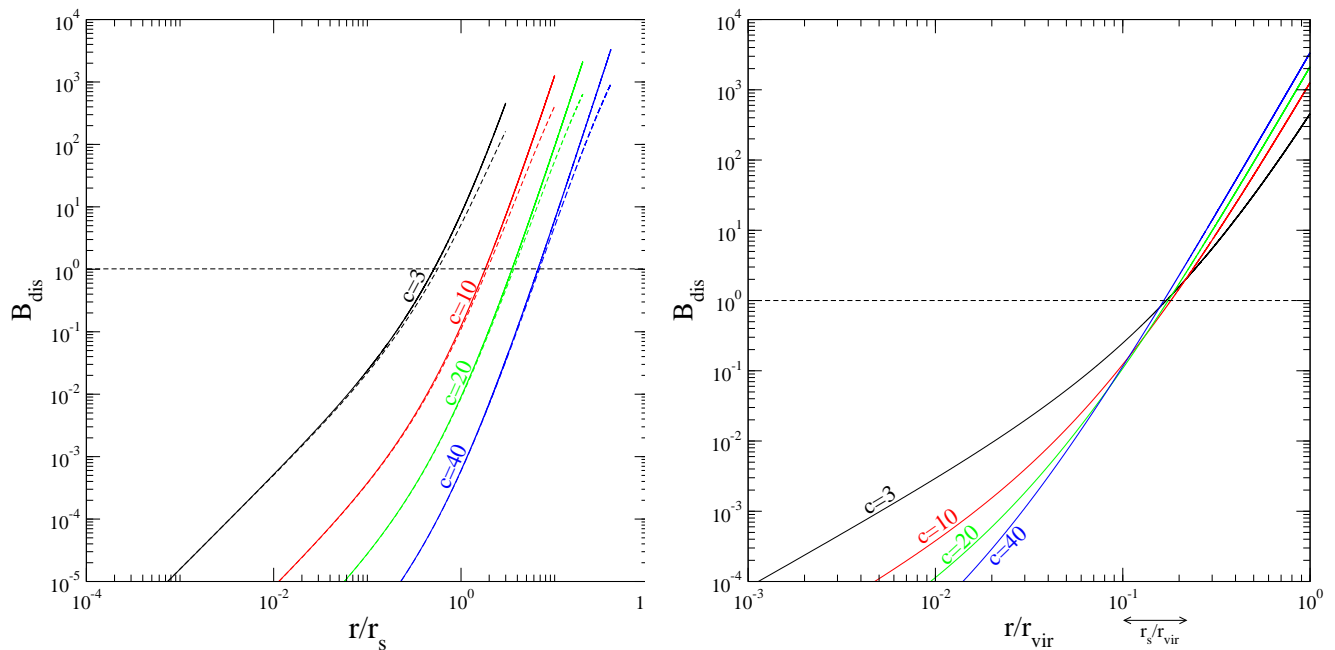


FIG. 4: The local boost factor due to primordial discreteness of the phase structure, for an NFW potential: The plots show how the boost in the annihilation measure of a DM halo changes as we go from the inner part of halo to outer parts, due to the discrete phase space structure of CDM. The local boost increases as we go towards the outskirts of the halo and also as we decrease the concentration. The dashed curves on the left panel show the boost if we include corrections due to a finite initial phase for the debris (68), which become important for nearly degenerate frequencies. The right panel shows that most of the boost comes from regions beyond 20% of the virial radius.

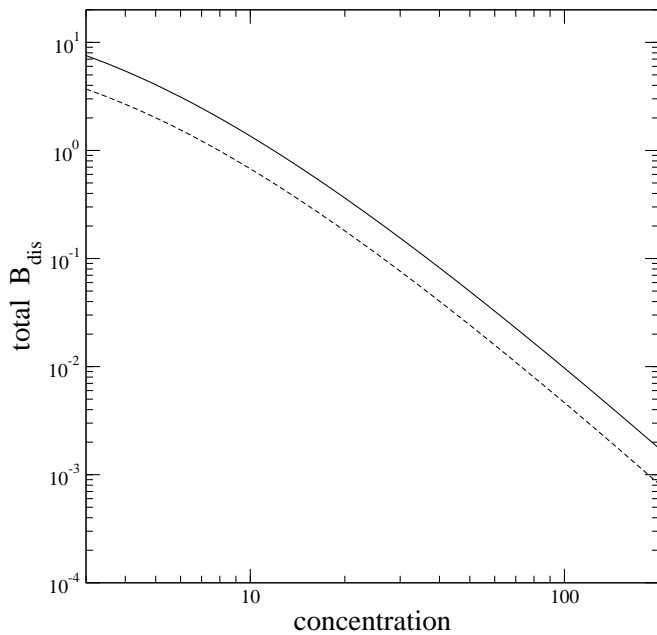


FIG. 5: The estimated total boost in the annihilation measure of a DM halo, due to the discrete distribution in the CDM phase space is shown for an NFW halo. The lower dashed curve shows the total boost when we include corrections due to a finite initial phase for the debris (68), which become important for nearly degenerate frequencies.

V. CONCLUSIONS

Working in phase space and with action-angle variables, we have shown that the density-density correlation function can capture the hierarchical phase structure of tidal debris and also the fundamental discreteness of the phase structure due to the coldness of the CDM initial conditions. The study presented here assumes no spherical symmetry, no continuous or smooth accretion, and no self-similar infall for the formation of dark matter haloes. It is thus a general scheme for quantifying the statistical properties of the phase structure of the virialized region of cosmological haloes.

As an application, we have obtained the significance for dark matter annihilation signal due to the hierarchical phase structure of tidal debris and have shown that this structure boosts the annihilation flux by order unity. On the other hand, the total boost due to the primordial discreteness of the phase space can be one order of magnitude higher for low-concentration (or recently formed) dark matter haloes.

While this paper dealt with unbound debris and caustics in dark matter haloes, in a companion paper [15], we calculate the boost to the annihilation signal due to the *gravitationally bound* substructure or sub-haloes. Combining the results of both papers, we can write down a concise and approximate formula for the local boost due

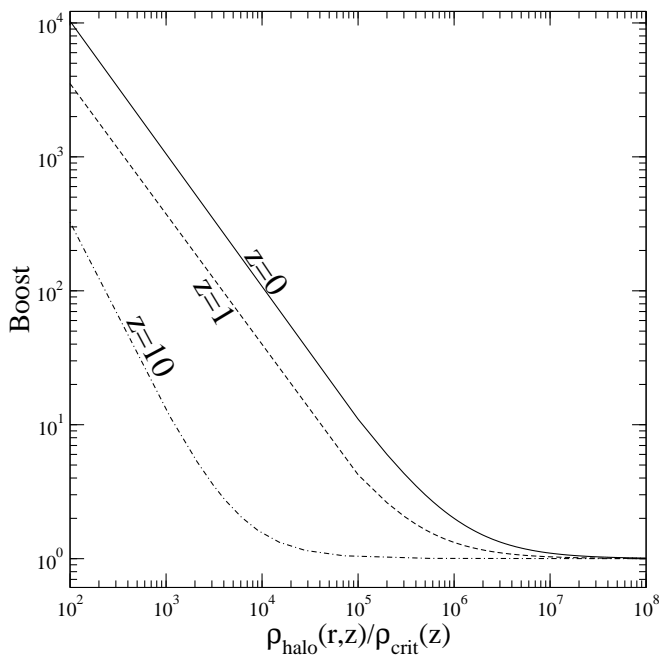


FIG. 6: The estimated local total boost including contributions from the debris, discreteness and the subhaloes, given by (69) with the first term set at its lowest value of unity, is shown for different redshifts. At high redshifts, the primordial caustics dominate over all other effects. However, at low redshifts the discreteness effect due to caustics is only important in the outskirts of the haloes.

to *all* substructures:

$$\text{Boost} \equiv \frac{\langle \rho^2(\mathbf{x}) \rangle}{\langle \rho(\mathbf{x}) \rangle^2} - 1 = B_{\text{debris}} + B_{\text{dis}} + B_{\text{sub}} \sim \mathcal{O}(1) + 3 \times 10^5 \left(\frac{\rho_{\text{crit}}}{\rho_{\text{halo}}(\mathbf{x})} \right)^{3/2} + 10^6 \left(\frac{\rho_{\text{crit}}}{\rho_{\text{halo}}(\mathbf{x})} \right) \left(\frac{H_0}{H} \right)^2, \quad (69)$$

which should be valid within a factor of 3 in the virialized region of the haloes. ρ_{halo} is the local coarse-grained density of the halo at redshift z , while ρ_{crit} is the critical density of the Universe at redshift z . The first term in (69) is due to the hierarchical structure of CDM debris, that we estimated in Sec. IV A. The second term is due to the discrete nature of the CDM phase space, where we used (59) with $\beta \sim 0.5$ and our nominal values for other parameters. Lastly, the third term is the contribution due to gravitationally bound sub-haloes [15]. We take

$H^2/H_0^2 = \Omega_m(1+z)^3 + \Omega_\lambda$ and plot (69) in Fig. 6.

One may wonder whether the discreteness of the phase space of sub-halos could lead to an additional boost in the annihilation signal. In other words, should we add B_{sub} and B_{dis} to get the total boost, or rather should they be multiplied? To answer this question, we notice that the main contribution to B_{sub} is due to the smallest sub-haloes (or micro-haloes) which have the highest densities [15], while the B_{dis} is mainly due to the lowest density regions of the haloes, which have the lowest degree of phase mixing. Therefore, we expect the two terms B_{sub} and B_{dis} to simply add incoherently, as the cross-correlation between the two sources of sub-structure should be small.

Finally, we should point out that the results here apply to phase structure within virial radius, and those outside the virial radius which we have not studied here, might yield a bigger boost factor. It is reasonable to study the streams and caustics that lie between the virial and the turnaround radii by using the secondary infall model [11], as radial approximation can be reasonably applied to regions beyond the virial radius (see Fig.4).

Finally, we remark on the most instrumental assumption in our framework, which was the integrability of orbits in the CDM potential, since one cannot define action-angle variables in a non-integrable system. This is characterized by the appearance of chaotic orbits in parts of the phase space. First, we should point out that as CDM haloes have a triaxial structure, a significant fraction of halo particles cannot be on chaotic orbits. Moreover, the difference between chaotic and integrable orbits only becomes important after many orbital times, which are only possible in the inner parts of the halo. As most of the boost to the annihilation caused by the discreteness in the action space comes from the outskirts of the halo (Fig.4), we do not expect a significant difference due to chaotic orbits. Nevertheless, the implications of chaos for the structure of the CDM phase space correlation function remains an intriguing question.

NA is supported by Perimeter Institute for Theoretical Physics. Research at Perimeter Institute is supported by the Government of Canada through Industry Canada and by the Province of Ontario through the Ministry of Research & Innovation. NA is grateful to IAP for hospitality. R.M. thanks French ANR (OTARIE) for grants and Perimeter Institute for hospitality. EB acknowledges support from NSF grant AST-0407050 and NASA grant NNG06GG99G.

-
- [1] S. Hofmann, D. J. Schwarz, and H. Stöcker, *PRD* **64** (Oct., 2001) 083507+, [arXiv:astro-ph/0104173](#).
[2] J. Diemand, B. Moore, and J. Stadel, *Nature* **433** (Jan., 2005) 389–391, [arXiv:astro-ph/0501589](#).
[3] E. Bertschinger, *Phys. Rev. D* **74** (Sept., 2006) 063509+, [arXiv:astro-ph/0607319](#).

- [4] P. Sikivie and J. R. Ipser, *Physics Letters B* **291** (Sept., 1992) 288.
[5] P. Sikivie, I. I. Tkachev, and Y. Wang, *Phys. Rev. D* **56** (Aug., 1997) 1863, [arXiv:astro-ph/9609022](#).
[6] A. Natarajan and P. Sikivie, *Phys. Rev. D* **73** (Jan., 2006) 023510+, [arXiv:astro-ph/0510743](#).

- [7] L. D. Duffy and P. Sikivie, *astro-ph/0805.4556* **805** (May, 2008) , 0805.4556.
- [8] S. D. M. White and M. Vogelsberger, *ArXiv e-prints* (Sept., 2008) , [arXiv:0809.0497](#).
- [9] R. A. Ibata, G. Gilmore, and M. J. Irwin, *Nature* **370** (July, 1994) 194–+.
- [10] A. Helmi, S. D. M. White, P. T. de Zeeuw, and H. Zhao, *Nature* **402** (Nov., 1999) 53–55, [arXiv:astro-ph/9911041](#).
- [11] J. A. Fillmore and P. Goldreich, *ApJ* **281** (June, 1984) 1–8.
- [12] E. Bertschinger, *ApJS* **58** (May, 1985) 39–65.
- [13] M. Vogelsberger, S. D. M. White, A. Helmi, and V. Springel, *MNRAS* **385** (Mar., 2008) 236–254, [arXiv:0711.1105](#).
- [14] J. Diemand and M. Kuhlen, *astro-ph/0804.4185* **804** (Apr., 2008) , 0804.4185.
- [15] N. Afshordi, R. Mohayaee, and E. Bertschinger, , *In preparation* .
- [16] S. Tremaine, *MNRAS* **307** (Aug., 1999) 877–883, [arXiv:astro-ph/9812146](#).
- [17] A. Helmi and S. D. M. White, *MNRAS* **307** (Aug., 1999) 495–517, [arXiv:astro-ph/9901102](#).
- [18] A. Helmi, S. D. M. White, and V. Springel, *MNRAS* **339** (Mar., 2003) 834–848.
- [19] P. J. McMillan and J. J. Binney, *astro-ph/0806.0319* **806** (June, 2008) , 0806.0319.
- [20] D. S. M. Fantin, M. R. Merrifield, and A. M. Green, *MNRAS* (Sept., 2008) 1091–+.
- [21] R. Mohayaee and P. Salati, *astro-ph/0801.3271* **801** (Jan., 2008) , 0801.3271.
- [22] R. Gavazzi, R. Mohayaee, and B. Fort, *A & A* **445** (Jan., 2006) 43–49, [arXiv:astro-ph/0506061](#).
- [23] C. Alard and S. Colombi, *MNRAS* **359** (May, 2005) 123–163, [arXiv:astro-ph/0406617](#).
- [24] J. Binney and S. Tremaine, *Galactic dynamics*. Princeton, NJ, Princeton University Press, 1987, 747 p., 1987.
- [25] C. J. Hogan, *PRD* **64** (Sept., 2001) 063515–+, [arXiv:astro-ph/0104106](#).
- [26] R. J. Scherrer and E. Bertschinger, *ApJ* **381** (Nov., 1991) 349–360.
- [27] A. Cooray and R. Sheth, *Phys. Rep.* **372** (Dec., 2002) 1–129, [arXiv:astro-ph/0206508](#).
- [28] R. Mohayaee and S. F. Shandarin, *MNRAS* **366** (Mar., 2006) 1217–1229, [arXiv:astro-ph/0503163](#).
- [29] J. F. Navarro, C. S. Frenk, and S. D. M. White, *ApJ* **490** (Dec., 1997) 493–+, [arXiv:astro-ph/9611107](#).